# Effect of Wood Flour Loading and Thermal Annealing on Viscoelastic Properties of Poly(lactic acid) Composite Films

**M. Hrabalova,[1] A. Gregorova,[2] R. Wimmer,[3] V. Sedlarik,[4,5] M. Machovsky,[4] N. Mundigler[1]**

[1]*Institute for Natural Materials Technology, Department for Agrobiotechnology, IFA-Tulln, University of Natural Resources and Applied Life Sciences, Vienna, A-1180, Austria*
[2]*Institute for Chemistry and Technology of Materials, Graz University of Technology, Graz 8010, Austria*
[3]*Faculty of Forest Sciences and Forest Ecology, University of Göttingen, Göttingen 37077, Germany*
[4]*Polymer Centre, Faculty of Technology, Tomas Bata University in Zlin, Zlin 76272, Czech Republic*
[5]*Jozef Stefan Institute, Jamova Cesta 39, 1000-Ljubljana, Slovenia*

Received 29 September 2008; accepted 25 March 2010
DOI 10.1002/app.32509
Published online 3 June 2010 in Wiley InterScience (www.interscience.wiley.com).

**ABSTRACT:** Poly(lactic acid) (PLA) films filled with up to 50 wt % softwood flour were prepared by melt compounding and thermocompression. Thermal annealing of the melt was performed at temperatures from 90°C to 120°C, for 45 min. Responses on polymer-filler interactions, viscoelastic properties, crystallinity of PLA as well as PLA-wood flour-filled films were investigated by differential scanning calorimetry (DSC), dynamic mechanical analysis (DMA), and scanning electron microscopy (SEM). The effectiveness of fillers on the storage moduli (C) was also calculated. The results reveal that wood flour (WF) in conjunction with thermal annealing affected the melting behavior of PLA matrix, and the glass transition temperature. It was further found that the effectiveness of the wood filler in biocomposites widely improved with thermal annealing as well as with higher WF concentration. Finally, it was found that the compatibility between WF and the PLA matrix can be improved when suitable annealing conditions are applied. © 2010 Wiley Periodicals, Inc. J Appl Polym Sci 118: 1534–1540, 2010

**Key words:** composites; viscoelastic properties; thermal properties; crystallization; annealing

## INTRODUCTION

Finding new applications of biodegradable polymeric materials for nonfood commodities and other products is a logical consequence of an increasing environmental awareness. The effort to decrease existing environmental load caused by the annually rising amount of plastic waste has been already considered in legislations.[1] As an example, European regulations for end-of-life vehicle recycling have created interest to look out for materials that are environmentally more compatible and biodegradable.[2] Biodegradable polymers may be divided into three groups: (1) Biopolymers of natural origin, (2) synthetic biodegradable polymers, and (3) modified polymeric materials to reach biodegradability.[3] Poly(lactic acid) (PLA) is a biodegradable, thermoplastic, aliphatic polyester, derived from renewable resources.[4,5] PLA has gained attention as a replacement for conventional synthetic polymeric packaging as well as construction materials during the past decade.[6,7] This biodegradable polymer has several drawbacks limiting its wider use in practice, which is brittleness, low-softening temperature, and the high price.[8] The existing problems have led to efforts to bring in PLA compatible modifiers, additives or fillers that improve mechanical properties, reduce cost of the final product and retain biodegradability at the same time.[9–12] Cellulose-derived fillers seem to meet all discussed demands and their potentialities are intensively investigated.[4,7,8,13–15] The reinforcing effect of the cellulose-based fibers improves mechanical and viscoelastic properties mainly the stiffness[7,11,16] due to the high strength of the fibers. Besides, cellulosic materials were chemically modified to improve the adhesion between the fiber surface and the polymer matrix,[7,12] which is poor due to the counter polarity of the substances. On the other hand, the interfacial performance of PLA-WF

*Correspondence to:* M. Hrabalova (marta.hrabalova@boku.ac.at).

Contract grant sponsor: Austrian Science Fund (FWF); contract grant number: L319-B16.
Contract grant sponsor: Austrian Ministry of Science and Technology and Ministry of Education, Youth and Sport of the Czech Republic; contract grant numbers: CZ 05/2009, MEB 060908.
Contract grant sponsor: Science and Education Foundation of the Republic of Slovenia (Program "Ad futura").

composite is also influenced by the transcrystalline region promoted on the fiber surface.[4,10,17] Generally, the physical constraints originating from the crystalline structure of the PLA, as well as other polymers, have crucial effect on the resulting macroscopic features including mechanical and thermal properties of PLA.[6,18–22] Crystal modifications of isothermally crystallized PLA were described by Zhang et al.[23] and its complex melting behavior by Yasuniwa et al.[24–26] It was proposed that the crystallization mechanism of PLA changes with the crystallization temperature.

On the basis of previously published observations, we hypothesize that the interfacial interaction between PLA and wood flour (WF) might be strongly dependent on the nature of PLA crystalline morphology, particularly on the thermal history of the composite and the number of nucleating sites in PLA. Dynamic mechanical analysis (DMA) was especially used as a highly sensitive method suitable for monitoring polymer-fiber interfaces[27] investigating changes introduced by different crystallization mechanisms as affected by the annealing temperature ($T_A$) during processing. Thermal and structural properties were also investigated by differential scanning calorimetry (DSC) and scanning electron microscopy (SEM), respectively.

## EXPERIMENTAL

### Materials

Poly(lactic acid) 7000D obtained from NatureWorks was used as the matrix material. The PLA was reinforced with commercially available softwood flour supplied by J. Rettenmaier & Söhne GmbH + Co., Germany. The softwood flour was ground and homogenized to finally pass a 120 μm sieve.

### Sample preparation

Polymer composites based on PLA and WF were prepared by melt mixing in a brabender kneader operating at 190°C and 20 rpm. PLA was first melted in the brabender and then mixed with the WF for 3 min. The composites were molded to thin films with a thickness of ~ 2.50 mm in a hot-press at 160°C preheated for 3 min before a pressure of 10 MPa was applied at 160°C for another 3 min. For thermal annealing, the molded films were kept in the temperature-controlled press for 45 min at a pressure of 10 MPa. Annealing temperatures were 90, 100, 110, and 120°C, respectively. Films were cooled down to room temperature by placing the molds into a cold press. The samples are designated as PLA_X_Y, with X indicating the wood flour concentration ($WF_c$) in wt %, and Y indicating the annealing temperature with a 0 for the unannealed samples. Before testing samples were conditioned for 1 week at 23°C and 50% relative humidity (RH).

### Differential scanning calorimetry

Thermal analysis was conducted on a Netzsch DSC 200 F3 Maja. Approximately 10 mg of sample was sealed in an aluminum pan. DSC scans were performed at a temperature range between −20°C and 180°C, at 10°C/min heating rate and a nitrogen gas flow of 60 mL/min. Melting temperatures ($T_m$) were determined from the melting peaks. Specific melting enthalpy ($\Delta H_m$) of the composites is referred to the actual mass fraction ($w$) of the PLA matrix and was calculated according to (1)

$$\Delta H_m = \frac{\Delta H_{m\exp} - \Delta H_c}{w} \quad (1)$$

where $\Delta H_c$ is the enthalpy of cold-crystallization, and $\Delta H_{m\exp}$ the heat of fusion obtained from the melting endotherm.[28]

### Dynamic-mechanical properties

Viscoelastic properties of neat PLA and the PLA-WF films included storage modulus ($E'$) as well as the loss factor $tan\ \delta = E''/E'$, with $E''$ being the loss modulus, both determined on a Netzsch DMA 242 C in tensile mode with strips 10 mm × 6 mm × 0.25 mm in size cut from the pressed films. Temperature range was varied between −10°C and +100°C. Measurements were accomplished at a strain sweep frequency of 1 Hz, and a heating rate of 3°C $min^{-1}$.

### Scanning electron microscopy

To visualize the effect of thermal annealing on the PLA-WF composites, i.e., the filler distribution and size, the films were also studied by thermionic-emission scanning electron microscopy (TESCAN VEGA/LMU). The surfaces were prepared by cryogenic fracturing in liquid nitrogen and then coated with a thin layer of Au/Pd. The microscope was operated under high-vacuum mode at an acceleration voltage of 5 kV.

## RESULTS AND DISCUSSION

### Thermal annealing and melting enthalpy

DSC records of the investigated samples revealed clear effects of thermal annealing as well as WF content on the melting behavior of the tested composites. In case of neat PLA, the expressed increase of $\Delta H_m$ as an indicator for polymer crystallinity was

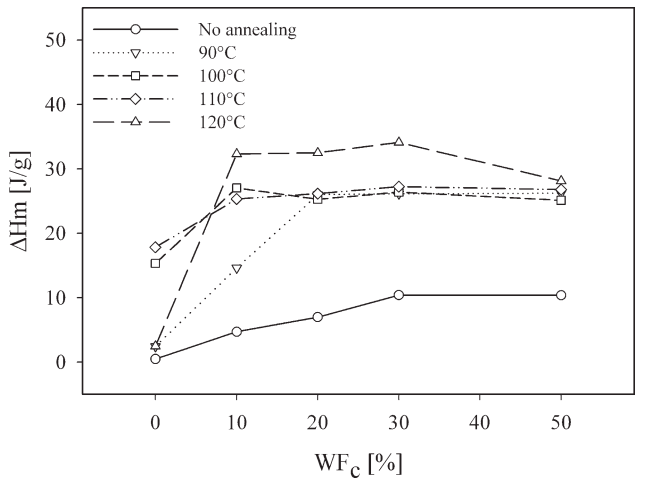


**Figure 1** Specific melting enthalpy of neat PLA and PLA-WF composites as related to wood flour content ($WF_c$) and the annealing temperature.

seen at annealing temperatures around of 100–110°C. The presence of the filler-induced changes in the melting enthalpy of the studied systems. The ability of WF to cause heterogeneous nucleation is proved by the substantial raise of $\Delta H_m$ along with increasing WF concentration. A nucleating effect of the WF filler is seen up to 30 wt % in the case of the unannealed composite. A large number of nucleating sites above this concentration has most likely led to a lack of space for spherulites, which impeded further advancement of the crystalline fraction.[29] Annealing had a pronounced influence on the observed $\Delta H_m$. As seen in Figure 1, the higher the annealing temperature, the higher the crystalline fraction present in the system. Melting enthalpy of composites annealed at $T_A = 120$°C was most expressed. Abe et al.[30] reported discontinuity in crystalline formation at about 120°C. Below this temperature, spherulite growth was evolved, and at higher, temperatures crystal thickening was favored. Thus, it can be proposed that higher $\Delta H_m$ might be a consequence of crystal thickening.

The synergism of both the nucleating ability of WF and the annealing temperature has led to highly crystalline material. For example, $\Delta H_m$ of PLA_10_120 was almost six times as high as unannealed PLA, both filled with 10% WF. With the addition of 10% WF, $\Delta H_m$ greatly responded at annealing temperatures of 90°C and 120°C. The $\Delta H_m$ response was less expressed at annealing temperatures of 100°C and 110°C, respectively. Melting enthalpy of the samples having flour fillings over 20 wt % seems not to be affected by thermal annealing. This indicates that the nucleating ability of WF above 20 wt % became ineffective. Consequently, the further development of the crystalline portion was affected by thermal annealing only.

Depending on preparation conditions, the three different crystalline modifications α, β, and γ of PLA are described.[31] The most common crystalline modification in melt-crystallized poly-L-lactic (PLLA) is the orthorhombic α-form and this modification is usually revealed at thermal annealing above 113°C. The crystalline modification formed below this temperature is not yet unambiguously clarified. Authors described the crystalline structure formed to be trigonal β-form;[31] on the other hand, it is also seen as a disordered α-form (pseudoorthorhombic).[24]

The influence of WF content and thermal annealing on melting endotherms is illustrated in Figure 2; thermal characteristics are summarized in Table I. The melting behavior of PLA is complex with regard to its multiple melting behavior as well as polymorphism and was intensively studied by several authors.[24,25,31–33] Yasuniwa et al. described the multiple melting behavior of PLA in dependence on crystallization temperature and stated the discrete change of melting and crystallization behavior (113°C).[31] In this study, a double melting behavior of PLA and PLA-WF, respectively, was observed for the sample sets annealed at $T_A < 110$°C. A low-temperature peak ($T_{m_1}$) located between 143°C and 149°C, and a high-temperature peak ($T_{m_2}$) between 151°C and 156°C was detected. The latter can be attributed to the melting of recrystallized crystals[26,33] (Table I). A shift of $T_{m_1}$ toward higher temperatures with higher $T_A$ was seen across the entire WF range. These results are in accordance with findings reported by Masirek et al.[11] For neat PLA films, the observed shift of $T_{m_1}$ might be due to crystalline growth along with $T_A$,[18,31] which is a consequence of concurrently declining nucleation rates. Therefore, $T_{m_1}$ of PLA can be described as melting of small

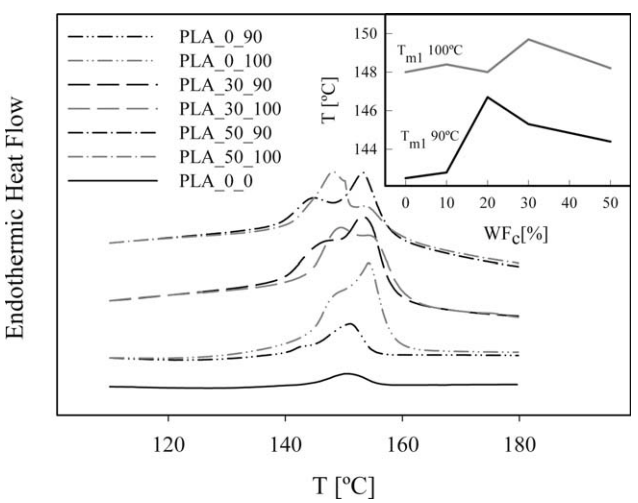


**Figure 2** DSC melting endotherms displaying double melting peak detection for $T_C = 90$°C and 100°C and $WF_c = 30$ and 50 wt % positive $T_{m_1}$ shift at higher $T_A$ is seen across the entire $WF_c$ range.

**TABLE I**
**Thermal Characteristics Derived from DSC Endotherms**

| | DSC[a] | | | | |
|---|---|---|---|---|---|
| Sample | $\Delta H_{m_1}$ (J/g) | $\Delta H_{m_2}$ (J/g) | $\Delta H_{m_1}/\Delta H_{m_2}$ | $\Delta T_{m_1}$ (°C) | $\Delta T_{m_2}$ (°C) |
| PLA_0_90 | 0.07 ± 0.01 | 4.59 ± 0.02 | 0.015 | 143 | 151 |
| PLA_0_100 | 0.77 ± 0.12 | 16.19 ± 0.23 | 0.048 | 148 | 154 |
| PLA_10_90 | 0.32 ± 0.03 | 18.62 ± 0.10 | 0.017 | 143 | 155 |
| PLA_10_100 | 2.55 ± 0.11 | 24.46 ± 0.18 | 0.104 | 148 | 155 |
| PLA_20_90 | 5.00 ± 0.40 | 20.96 ± 0.22 | 0.239 | 147 | 156 |
| PLA_20_100 | 2.63 ± 0.34 | 22.62 ± 0.37 | 0.116 | 148 | 153 |
| PLA_30_90 | 5.16 ± 0.30 | 20.94 ± 0.29 | 0.246 | 145 | 153 |
| PLA_30_100 | 3.75 ± 0.30 | 22.60 ± 0.29 | 0.166 | 149 | 155 |
| PLA_50_90 | 6.34 ± 0.30 | 19.86 ± 0.68 | 0.319 | 144 | 153 |
| PLA_50_100 | 9.36 ± 0.45 | 15.73 ± 0.55 | 0.595 | 148 | 154 |

[a] Standard deviations were based on triple DSC measurement evaluations.

crystallites having low-thermal stability.[33] For WF-filled samples, a $T_{m_1}$ shift might be the combination of crystalline growth and lamellar thickening of transcrystalline region.[34] For $T_A \geq 110$°C, low-temperature peak $T_{m_1}$ has merged with the $T_{m_2}$ peak at 153–155°C. Melting temperature of the neat PLA was seen at 151°C. The absence of an exothermic peak between $T_{m_1}$ and $T_{m_2}$ indicates that the rate of recrystallization has overwhelmed the rate of melting.[32] As shown in Table I, the area ratio of the low-temperature peak to the high-temperature peak ($\Delta H_{m_1}/\Delta H_{m_2}$) increased with $WF_c$ at each $T_A$. This contribution for $\Delta H_m$ of the low-temperature peak can be explained by a tendency of transcrystalline region development at the PLA-WF interface.[16] Accordingly, the advancement of the area of the low-temperature peak might be caused by the melting at the transcrystalline region, which was markedly extended at higher $WF_c$.

## Viscoelastic properties

Effects of WF content and thermal annealing on the storage moduli ($E'$) in at the glassy and rubbery region (20°C and 80°C, respectively) are listed in Table II. As seen in Figure 3, the capability of the composites to store mechanical energy and resist deformation has increased as WF gets incorporated. This is due to higher rigidity of the filler and the reinforcing effect in the PLA matrix.[35–39] $E'$ in the glassy region was not susceptible to thermal annealing with exception of higher WF loaded samples at 110°C (PLA_30_110 and PLA_50_110). By contrast, the rubbery region of the composites was considerably affected by thermal annealing as a result of the improved thermal stability.[15] The improvement of $E'$ was paralleled with higher $WF_c$. This effect was expressed by the factor $C$, which is the effectiveness of the filler on $E'$ in a given polymer matrix:[38]

$$C = \frac{(E'_g/E'_r)_{\text{comp}}}{(E'_g/E'_r)_{\text{matrix}}} \quad (2)$$

where $E'_g$ and $E'_r$ are storage moduli measured in the glassy and the rubbery regions, at a sweep frequency of 1 Hz. The factor $C$ is inversely proportional to the filler effectivity in the composite. Lower the $C$, higher the effectiveness of the filler on the composite storage modulus. The effectiveness of the

**TABLE II**
**Variation of Glass Transition Temperature, Loss Factor, and Storage Moduli in Glassy and Rubbery State, with $WF_c$ and Annealing Temperature**

| | $T_g$ (°C) | *tan* δ | $E'$ at 20°C (GPa) | $E'$ at 80°C (GPa) |
|---|---|---|---|---|
| PLA_0_0 | 63 | 2.307 | 2.59 | 0.025 |
| PLA_0_90 | 63 | 2.123 | 2.157 | 0.080 |
| PLA_0_100 | 65 | 0.709 | 2.487 | 0.065 |
| PLA_0_110 | 63 | 1.336 | 2.309 | 0.019 |
| PLA_0_120 | 63 | 1.890 | 2.345 | 0.029 |
| PLA_10_0 | 65 | 1.989 | 2.694 | 0.013 |
| PLA_10_90 | 64 | 0.477 | 2.564 | 0.138 |
| PLA_10_100 | 70 | 0.224 | 2.598 | 0.483 |
| PLA_10_110 | 65 | 0.217 | 2.701 | 0.527 |
| PLA_10_120 | 67 | 0.219 | 2.757 | 0.599 |
| PLA_20_0 | 64 | 1.462 | 2.654 | 0.035 |
| PLA_20_90 | 66 | 0.236 | 3.185 | 0.637 |
| PLA_20_100 | 68 | 0.195 | 2.773 | 0.618 |
| PLA_20_110 | 65 | 0.205 | 2.818 | 0.603 |
| PLA_20_120 | 65 | 0.180 | 2.83 | 0.707 |
| PLA_30_0 | 64 | 1.204 | 3.057 | 0.053 |
| PLA_30_90 | 68 | 0.177 | 3.661 | 0.984 |
| PLA_30_100 | 68 | 0.164 | 3.802 | 1.169 |
| PLA_30_110 | 65 | 0.190 | 4.502 | 1.008 |
| PLA_30_120 | 64 | 0.174 | 3.087 | 0.750 |
| PLA_50_0 | 68 | 0.631 | 3.883 | 0.143 |
| PLA_50_90 | 67 | 0.155 | 4.012 | 1.328 |
| PLA_50_100 | 71 | 0.146 | 3.855 | 1.546 |
| PLA_50_110 | 65 | 0.137 | 5.972 | 1.941 |
| PLA_50_120 | 66 | 0.129 | 3.713 | 1.364 |

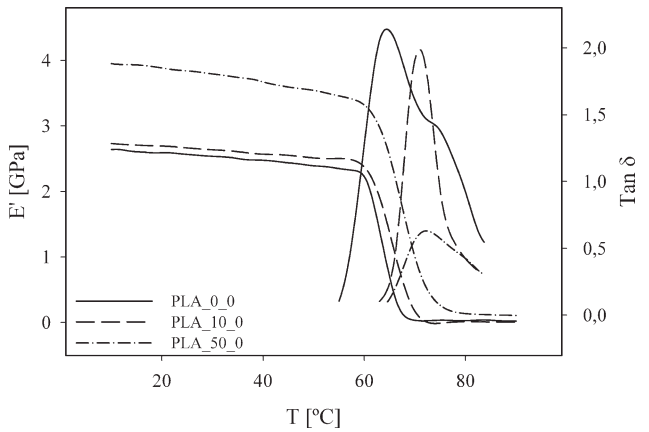


**Figure 3** Storage modulus and *tan* δ as related to temperature measured for unannealed PLA films containing 0, 10, and 50% of WF. Reduced *tan* δ peaks as well as improved storage moduli are going along with higher $WF_c$.

filler on $E'$ of nonannealed PLA-WF film was lowest for the system with 10% WF loading and highest for the 50% WF loading. As seen in Figure 4, the $C$ factor dropped with increasing $WF_c$ and $T_A$, but only up to a $T_A$ of 110°C. Results confirm the thermal stability in the rubbery region, which is caused by WF with reference to thermal annealing. The stress transfer between WF and the matrix weakened at $T_A = 120$°C (see Fig. 3).

The maximum rate of turndown of the $E'$ was attributed to the glass transition temperature (Table II). Although the $T_g$ of unfilled unannealed samples is not susceptible to thermal annealing, $T_g$ of WF reinforced samples moved to higher temperatures as a consequence of restricted dynamics of polymer chains in confined environments.[39]

Loss factor (*tan* δ) is an indicator for mechanical damping or internal friction in a viscoelastic system.[38] In composites, a lower *tan* δ indicates better interfacial bonding between filler and matrix.[27,38] The highest *tan* δ was measured for neat, unannealed PLA. As seen in Table II, *tan* δ is inversely proportional to $WF_c$ for a given annealing temperature.[27] The restriction of molecular chain movements is driven by two factors: (1) matrix crystallinity[40] and (2) presence of WF. The crystalline portions in PLA matrices filled with 20–50% wood fibers, annealed at $T_A = 90$–100°C, turned out to be constant, whereas though *tan* δ decreased within the same $T_A$ range. This indicates improved interaction between filler and matrix as a consequence of different polymer states in connection with filler particles.[37] It is assumed that transcrystalline growth within annealing temperature range of 90–100°C has improved interfacial bonding between fiber and the matrix.

### Scanning electron microscopy

Fracture surfaces of unannealed PLA composites filled with 10% WF [Fig. 5(a)] showed a relatively smooth surface with WF particles having 20 μm in length and about 10 μm in thickness. The effect of thermal annealing is clearly seen in Figure 5(b). The fracture surface appeared fissured, which reveals the higher brittleness of the material. The fracture surface of the composite with the highest investigated WF content, unannealed and annealed, is seen in Figure 5(c) (PLA_50_0) and Figure 5(d) (PLA_50_120), respectively. The highly filled PLA composites are characteristic by a dense and uniform distribution of WF particles within the polymer matrix. The microstructure of the cold fracture of annealed PLA_50_120, which had significantly higher crystallinity than the unannealed comparison (PLA_50_0), shows considerable higher level of WF-PLA matrix isolation. This was most likely caused by the rigidity of the polymer due to organization of the polymeric chains into geometric units. This has led to a loss of the polymer-filler cohesion as seen in the presented SEM pictures. The obtained results are in coherence with the increased $C$ factor, as determined through DMA.

## CONCLUSIONS

In this study, PLA—wood fiber composites were subjected to thermal annealing to observe the effects on different properties. Results revealed that WF in conjunction with thermal annealing had strong effects on the melting behavior of PLA matrix, and also on the glass transition temperature. Overall, compatibility between WF and the PLA matrix was improved under suitable annealing conditions. It

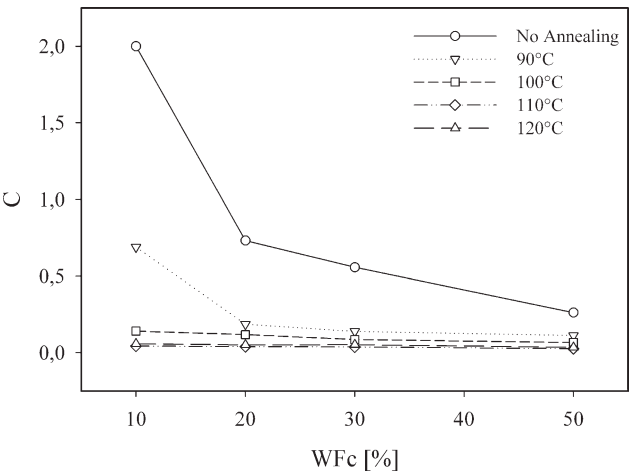


**Figure 4** Constant $C$ versus $WF_c$ for different annealing temperatures.

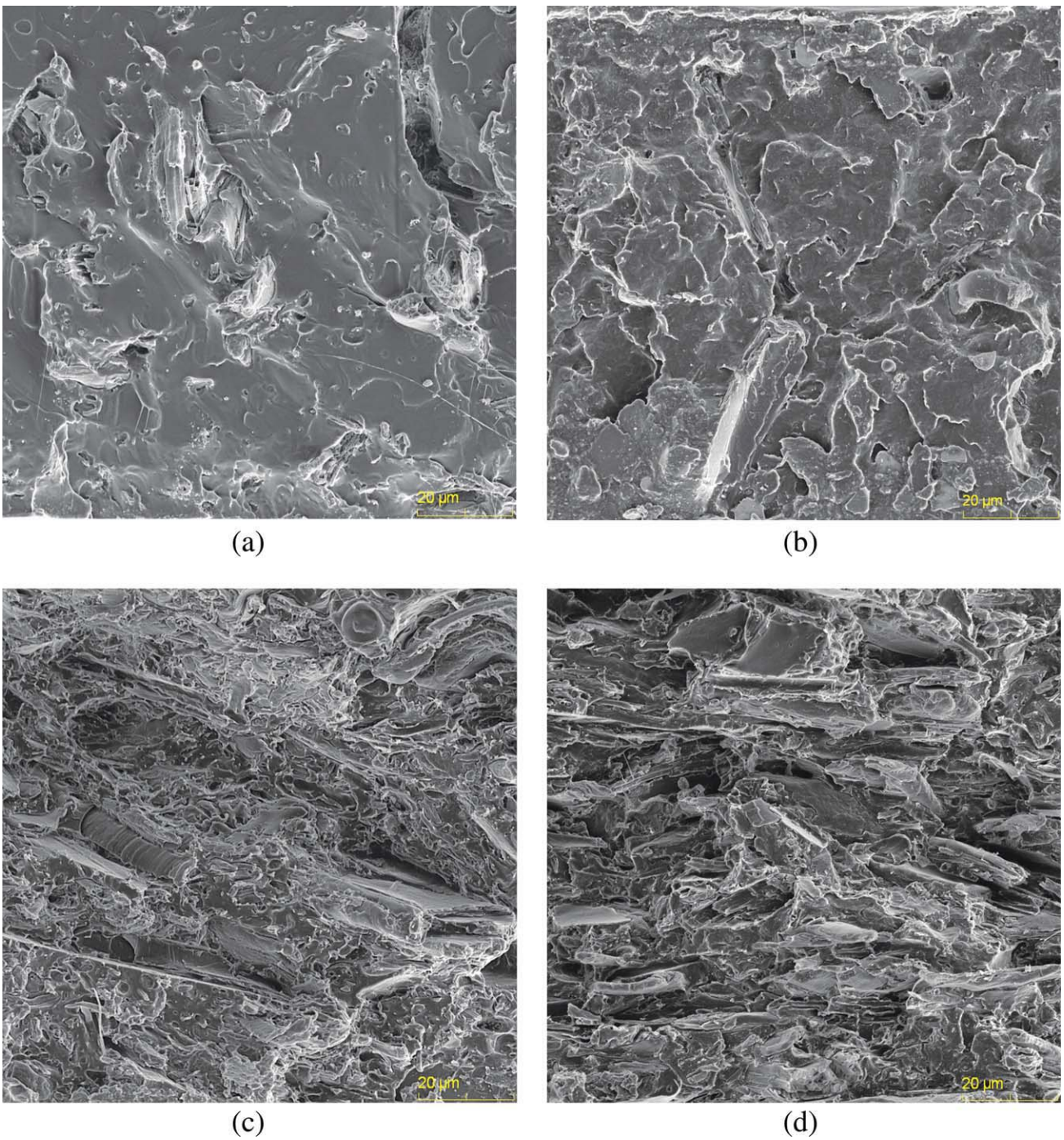


**Figure 5** SEM micrographs of fracture surfaces. (a) PLA_10_0 (10% wood fibers, unannealed), (b) PLA_10_120 (10% wood fibers, 120°C annealing, (c) PLA_50_0 (50% wood fibers, unannealled, and (d) PLA_50_120 (50% wood fibers, 120°C annealing). [Color figure can be viewed in the online issue, which is available at www.interscience.wiley.com.]

was found that WF, in conjunction with applied annealing, is both instrumental to influence the crystalline structure of a PLA composite. Therefore, to optimize fiber-matrix compatibility, the crystallization mechanisms need to be better considered in the processing of wood fiber filled PLA composites. With suitable crystalline structure, wood filler content as well as processing conditions, the property profiles of PLA-based composites can be optimized.

## References

1. Scott, G. In Degradable Polymers. Principles and Applications; Scott, G., Ed.; Kluwer Academic Publishers: Netherlands, 2002; p 1.
2. Heyde, M. Polym Degrad Stab 1998, 59, 3.
3. Hartmann, M. H. In Biopolymers from Renewable Resources; Kaplan, D. L., Ed.; Springer Academic Press: Berlin, 1998; Vol. 15, p 367.
4. Mathew, A. P.; Oksman, K.; Sain, M. J Appl Polym Sci 2005, 97, 2014.

5. Sedlarik, V.; Saha, N.; Sedlarikova, J.; Saha, P. Macromol Symp 2008, 272, 100.
6. Garlotta, D. J Polym Environ 2001, 9, 63.
7. Huda, M. S.; Drzal, L. T.; Mohanty, A. K.; Misra, M. Compos Sci Technol 2006, 66, 1813.
8. Sedlarik, V.; Saha, N.; Kuritka, I.; Saha, P. J Appl Polym Sci 2007, 106, 1869.
9. Wang, H.; Sun, X.; Seib, P. J Appl Polym Sci 2002, 84, 1257.
10. Pilla, S.; Gong, S.; Neill, E. O.; Rowell, R. M.; Krzysik, A. M. Polym Eng Sci 2008, 48, 578.
11. Masirek, R.; Kulinski, Z.; Chionna, D.; Piorkowska, E.; Pracella, M. J Appl Polym Sci 2007, 105, 255.
12. Gregorova, A.; Hrabalova, M.; Wimmer, R.; Saake, B.; Altaner, C. J Appl Polym Sci 2009, 114, 2616.
13. Sedlarik, V.; Saha, N.; Saha, P. Polym Degrad Stab 2006, 91, 2039.
14. Sedlarik, V.; Saha, N.; Kuritka, I.; Emri, I.; Saha, P. Plast Rubber Compos 2006, 35, 355.
15. Julinova, M.; Kupec, J.; Alexy, P.; Hoffmann, J.; Sedlarik, V.; Vojtek, T.; Chromcakova, J.; Bugaj, P. Polym Degrad Stab 2010, 95, 225.
16. Huda, M. S.; Drzal, L. T.; Mohanty, A. K.; Misra, M. Compos Sci Technol 2008, 68, 424.
17. Mathew, A. P.; Oksman, K.; Sain, M. J Appl Polym Sci 2006, 101, 300.
18. Tsuji, H.; Ikada, Y. Polymer 1995, 36, 2709.
19. Junkar, I.; Cvelbar, U.; Vesel, A.; Hauptman, N.; Mozetic, M. Plasma Process Polym 2009, 6, 667.
20. Junkar, I.; Vesel, A.; Cvelbar, U.; Mozetic, M.; Strnad, S. Vacuum 2009, 84, 83.
21. Vesel, A.; Junkar, I.; Cvelbar, U.; Kovac, J.; Mozetic, M. Surf Interface Anal 2008, 40, 1444.
22. Vesel, A.; Mozetic, M.; Zalar, A. Surf Interface Anal 2008, 40, 661.
23. Zhang, J.; Duan, Y.; Sato, H.; Tsuji, H.; Noda, I.; Yan, S.; Ozaki, Y. Macromolecules 2005, 38, 8012.
24. Yasuniwa, M.; Tsubakihara, S.; Sugimoto, Y.; Nakafuku, C. J Appl Polym Sci Part B: Polym Phys 2004, 42, 25.
25. Yasuniwa, M.; Iura, K.; Dan, Y. Polymer 2007, 48, 5398.
26. Yasuniwa, M.; Sakamo, K.; Ono, Y.; Kawahara, W. Polymer 2008, 49, 1943.
27. Keusch, S.; Haessler, R. Compos A 1999, 30, 997.
28. Sedlarik, V.; Kucharczyk, P.; Kasparkova, V.; Drbohlav, J.; Salkova, A.; Saha, P. J Appl Polym Sci 2010, 116, 1597.
29. Moon, C. K. J Appl Polym Sci 1998, 67, 1191.
30. Abe, H.; Kikkawa, Z.; Inoue, Y.; Doi, Y. Biomacromolecules 2001, 2, 1007.
31. Yasuniwa, M.; Tsubakihara, S.; Iura, K.; Ono, Y.; Dan, Y.; Takahashi, K. Polymer 2006, 47, 7554.
32. Yasuniwa, M.; Tsubakihara, S.; Fujioka, T. Thermochim Acta 2003, 396, 75.
33. Di Lorenzo, M. L. Macromol Symp 2006, 234, 176.
34. Ninomiya, N.; Kato, K.; Fujimori, A.; Masuko, T. Polymer 2007, 48, 4874.
35. Huda, M. S.; Drzal, L. T.; Misra, M.; Mohanty, A. K. J Appl Polym Sci 2006, 102, 4856.
36. Huda, M. S.; Mohanty, A. K.; Misra, M.; Drzal, L. T.; Schut, E. J Mater Sci 2005, 40, 4221.
37. Jamil, M. S.; Ahmad, I.; Abdullah, I. J Polym Res 2006, 4, 315.
38. Pothan, L. A.; Oommen, Z.; Thomas, S. Compos Sci Technol 2003, 63, 283.
39. Zuza, E.; Ugartemendia, J. M.; Lopez, A.; Meaurio, E.; Lejardi, A.; Sarasua, J. R. Polymer 2008, 49, 4427.
40. Chiellini, E.; Covolan, V. L.; Lorenzo, M.; Solaro, E. Macromol Symp 2003, 97, 345.